ELSEVIER

Journal of Materials Processing Technology 177 (2006) 114–120

Journal of Materials Processing Technology

www.elsevier.com/locate/jmatprotec

Analysis of asymmetrical cold and hot bond rolling of unbounded clad sheet under constant shear friction

S.C. Pan [a], M.N. Huang [b,*], G.-Y. Tzou [b], S.W. Syu [b]

[a] *Department of Architectural Engineering, Yung-Ta Institute of Technology, Ping-Tung, Taiwan, ROC*
[b] *Department of Mechanical Engineering, Yung-Ta Institute of Technology, Ping-Tung, Taiwan, ROC*

Abstract

An analytical model for asymmetrical cold and hot bond rolling of two-layer unbounded clad sheet unbounded before rolling is derived to investigate the stress field using a direct formulation. Constant shear friction between the rolls and the clad sheet is assumed. Due to different roll speeds and roll radii, two neutral points and one bonding point are generated at the roll gap; the plastic deformation regions can be divided into four zones. The neutral points, the rolling pressure distribution, the horizontal stress of the whole clad sheet, the horizontal stresses in the component layers, the shear stress at the interface, the rolling force, and the rolling torque, can be easily and rapidly calculated. The determination of the bonding point and the clad thickness ratio at the exit are of great important. The results obtained from this study have been compared with experiment [Y.M. Huang, T.H. Chen, H.H. Hsu, Analysis of asymmetrical clad sheet rolling by stream function method, Int. J. Mech. Sci. 38 (1996) 443–460] to verify the feasibility of the model.

Keywords: Bond rolling; Bonding point; Neutral point; Thickness ratio of clad sheet

1. Introduction

Studies concerning clad sheet rolling can be divided into experimental studies [1,2] and theoretical studies [3–13]. Lee and Lee [2] performed cold roll bonding for silver and phosphor bronze sheets under the same roll radii, and analysis assuming Coulomb friction together with the Runge–Kutta numerical method to obtain the rolling pressure and thickness ratio of clad sheet at the exit. The CPU time required is too great to obtain more detailed information. Suzuki et al. [3,4] used the slab method and the Runge–Kutta method to obtain the stress field, assuming Coulomb friction. Kiuchi and Hwang [5,6] used the upper bound method to explore the plastic deformation of clad sheet, assuming constant shear friction. Hwang et al. [7,8] used the upper bound method and stream function method to establish the mathematical model and perform the experiment. Jiang et al. [9] referred to Hwang's paper [8] to develop the simplified model based on the upper bound model. However, the stress field of clad sheet cannot be obtained by the upper bound method and stream function method. Hamauzu [10] and Shiyouya [11] used FEM to investigate the effects of thickness ratio and shear yield stress ratio on the effective stress and strain, rolling force. Luo et al. [12] used the rigid-plastic finite-element formulation for slightly compressible materials to examine the behavior of bonding. The CPU time required by the mentioned methods is more so as not to be suitable for on-line rolling industry applications to predict rolling force and torque. For determining rolling pressure, rolling force and rolling torque, the slab method is a good technique if without using Runge–Kutta method. Although Suzuki used the slab method with Coulomb friction to establish his analytical model, the Runge–Kutta method was still used to solve the solution. Thus, in this study a new analytical approach to asymmetrical cold and hot bond rolling of clad sheet unbounded before rolling is developed to get the various stress distributions easily and rapidly without Runge–Kutta numerical method under constant shear friction.

2. Modeling

Fig. 1 shows a schematic illustration of asymmetrical bond rolling of clad sheet. Assuming the radius and speed of the upper roll are different from those of the lower roll. The plastic deformation region at the roll gap is divided into four distinct regions.

* Corresponding author.
E-mail address: tzougowyi@yahoo.com.tw (M.N. Huang).

0924-0136/$ – see front matter © 2006 Elsevier B.V. All rights reserved.
doi:10.1016/j.jmatprotec.2006.04.071

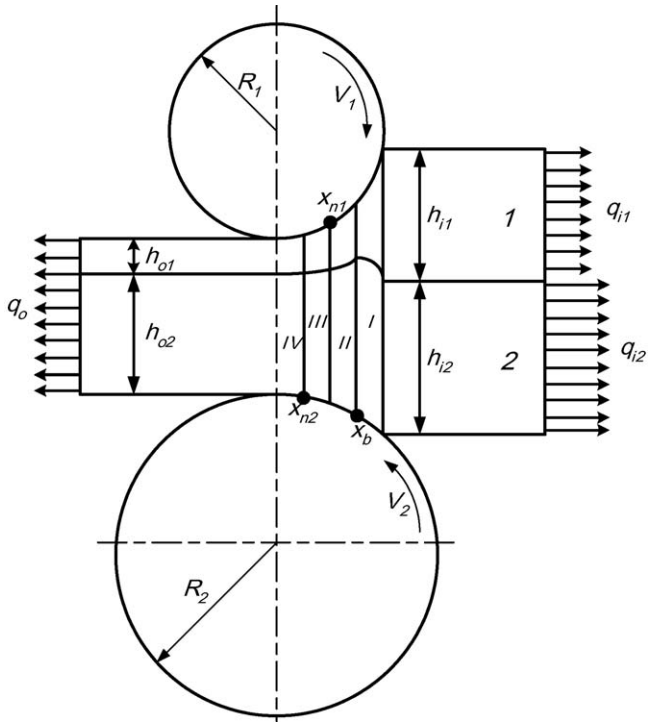

Fig. 1. Schematic illustration of asymmetrical bond rolling of clad sheet.

Due to the clad sheet being unbounded before rolling, as the unbounded clad sheet is initially bit into the roll gap, the soft sheet (layer 1) is yielded, however, the hard sheet (layer 2) is not yet yielded. Thus, this region (zone I) belongs to the unbounded region. The slab stress state in zone I is shown in Fig. 2, where the shear stress at the interface (τ_m) is assumed as m_3k_1, k_1 being the mean yield shear stress of the soft layer. As the harder sheet is yielded, the clad sheet is bonded completely, the bonding point (x_b) is generated. The plastic deformation region at the roll gap can be divided into four distinct regions, zone I ($x_b \le x \le L$) for the unbounded region; zone II ($x_{n1} \le x \le x_b$), zone III ($x_{n2} \le x \le x_{n1}$) and zone IV ($0 \le x \le x_{n2}$) for the bounded regions. The slab state of the clad sheet in zone II is shown in Fig. 3, zone III is the cross shear region where the frictional shear stresses are reverse, and the frictional shear stresses in zone IV are opposite to that in zone II. Zone II, III, and IV for the shear stress at the interface (τ_m) should be determined by the model. Zone I is the region of the unbounded clad sheet, where the soft sheet (layer 1) is yielded with the yield criterion $p + q = 2k_1$, but the hard sheet (layer 2) is not yielded, which means $p + q_2 < 2k_2$. Thus the governing equation for the soft sheet has to be established first.

2.1. Zone I ($x_b \le x \le L$), $\tau_e = m_1k_1 + m_2k_2$

Because the hard sheet (layer 2) is not yielded, means the contact angle (θ_m) at the interface equals the contact angle (θ_2) between roll and clad sheet in zone I ($x_b \le x \le L$). The thickness (h) in zone I is equal to $h_1 + h_{i2}$. It indicates the thickness of the hard sheet in zone I ($h_2 = h_{i2}$) has not been changed.

For soft sheet (layer 1): $p + q_1 = 2k_1$; $dq_1 = -dp$.

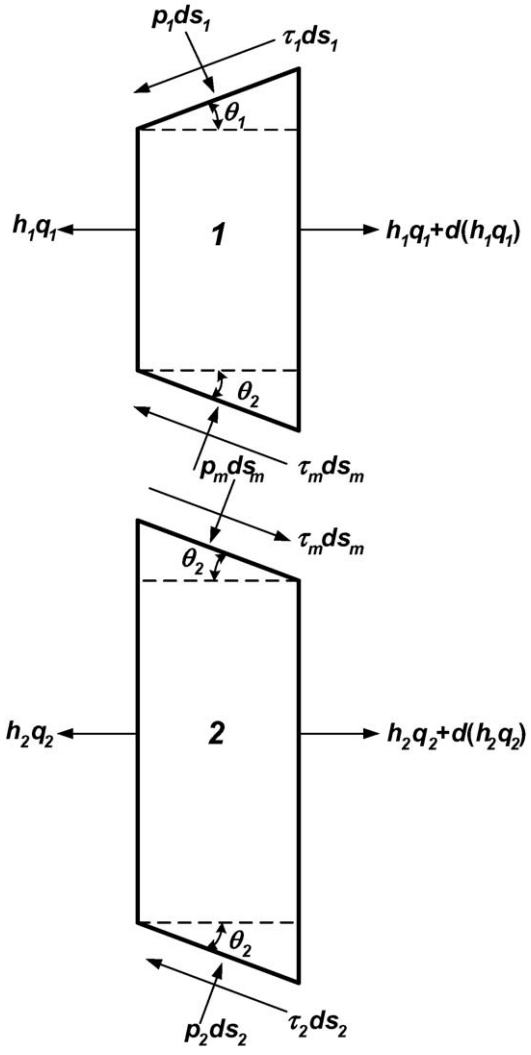

Fig. 2. Slab stress state of unbounded clad sheet in zone I.

Combining the horizontal and vertical force equilibrium equations; then becomes:

$$\frac{d(h_1q_1)}{dx} + p(\tan\theta_1 + \tan\theta_m) - \tau_1(\tan^2\theta_1 + 1) - \tau_m(\tan^2\theta_m + 1) = 0 \quad (1)$$

where

$$\tan\theta_1 = \frac{x}{R_1}, \quad h = h_o + \frac{x^2}{R_{eq}} = h_1 + h_{i2},$$

$$\frac{dh}{dx} = \frac{dh_1}{dx} = \frac{2x}{R_{eq}}, \quad \tau_1 = m_1k_1, \quad \tau_m = m_3k_1$$

By using the von Mises yield criterion, geometrical conditions, and frictional conditions, Eq. (1) becomes:

$$\frac{dp}{dx} = \frac{A_1}{x^2 + R_{eq}(h_o - h_{i2})}x^2 + \frac{4k_1}{x^2 + R_{eq}(h_o - h_{i2})}x - \frac{R_{eq}(m_3k_1 + m_1k_1)}{x^2 + R_{eq}(h_o - h_{i2})} \quad (2)$$

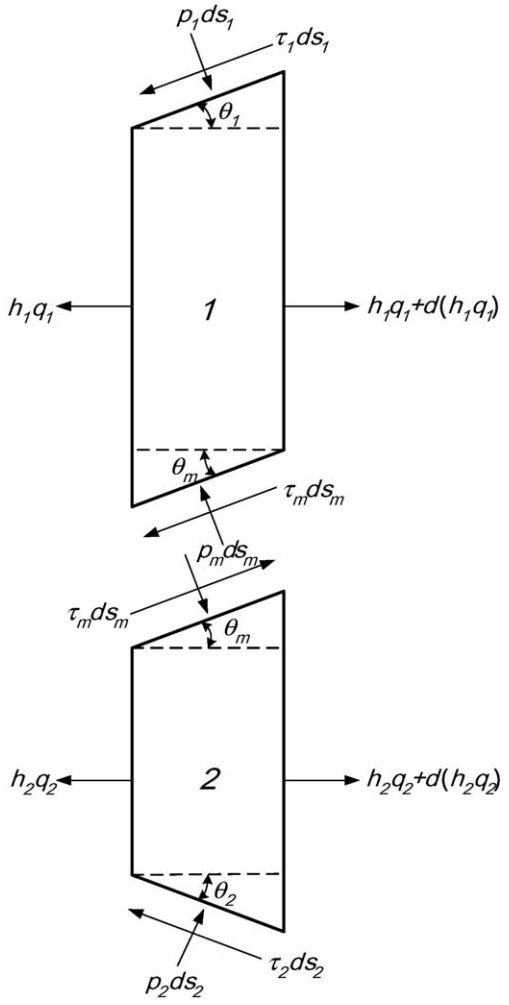

Fig. 3. Slab stress state of clad sheet in zone II.

where

$$A_1 = -R_{eq} k_1 \left(\frac{m_1}{R_1^2} + \frac{m_3}{R_2^2} \right)$$

The rolling pressure distribution in zone I (p_I) can be solved from Eq. (2) as follows:

$$p_I = A_1 x + B_1 \ln(x^2 + D_1) + C_1 \omega_1 + c_1^* \tag{3}$$

where

$$A_1 = -R_{eq} k_1 \left(\frac{m_1}{R_1^2} + \frac{m_3}{R_2^2} \right),$$

$$B_1 = 2k_1, \quad C_1 = -\left[A_1 \sqrt{D_1} + \frac{R_{eq} k_1 (m_3 + m_1)}{\sqrt{D_1}} \right],$$

$$D_1 = R_{eq}(h_o - h_{i2}), \quad \omega_1 = \tan^{-1} \frac{x}{\sqrt{D_1}}$$

For the hard sheet (layer 2): $p + q_2 < 2k_2$, $h_2 = h_{i2}$, $dh_2/dx = 0$.

Similarly, combining the horizontal and vertical force equilibrium equations, then gives:

$$\frac{dq_2}{dx} = \frac{(\tau_2 - \tau_m)}{h_{i2}} \left(\frac{x^2}{R_2^2} + 1 \right) \tag{4}$$

where $\tau_2 = m_2 k_2$.

The horizontal stress of layer 2 (q_2) can be derived from:

$$q_2 = E_1 x^3 + F_1 x + c_q^* \tag{5}$$

where

$$E_1 = \frac{F_1}{3R_2^2}, \quad F_1 = \frac{m_2 k_2 - m_3 k_1}{h_{i2}}$$

c_1^* and c_q^* have to be determined by the boundary conditions.

Boundary conditions:

(1) At $x = L$ (or $\omega = \omega_{i1}$), $q_1 = q_{i1}$, $p_i = 2k_1 - q_{i1}$.
c_1^* in Eq. (3) can be obtained:

$$c_1^* = 2k_1 - q_{i1} - A_1 L - B_1 \ln(L^2 + D_1) - C_1 \omega_{i1} \tag{6}$$

where

$$C_1 = -\left[A_1 \sqrt{D_1} + \frac{R_{eq} k_1 (m_3 + m_1)}{\sqrt{D_1}} \right],$$

$$\omega_{i1} = \tan^{-1} \frac{L}{\sqrt{D_1}}$$

(2) At $x = L$ (or $\omega = \omega_{i1}$), $q_2 = q_{i2}$.
c_q^* in Eq. (5) is can be obtained from:

$$c_q^* = q_{i2} - E_1 L^3 - F_1 L \tag{7}$$

(3) Determination of the bonding point (x_b).
At $x = x_b$, the hard sheet is just yielded, so the yield criterion is $p + q_2 = 2k_2$. By using the yield criterion, the equations for determining the bonding point are obtained from:

$$A_1 x_b + B_1 \ln(x_b^2 + D_1) + C_1 \omega_{b1} + c_1^* + E_1 x_b^3 + F_1 x_b + c_q^* = 2k_2 \tag{8}$$

where

$$\omega_{b1} = \tan^{-1} \frac{x_b}{\sqrt{D_1}}$$

x_b can be easily solved using the bisection method.

The specific shear stress $(\tau_m/k_1)_I$ in zone I can be obtained as:

$$\left(\frac{\tau_m}{k_1} \right)_I = m_3 \tag{9}$$

2.2. Zone II ($x_{n1} \le x \le x_b$), $\tau_e = m_1 k_1 + m_2 k_2$

In zone II, two component layers have been bonded, but the thickness ratio of clad sheet at the entrance and exit are different,

that is, $\beta_i = h_{i1}/h_1$ and $\beta_o = h_{b1}/h_b = h_{o1}/h_o$. In other word, β_o should not be equal to β_i.

The rolling pressure distribution in zone II is expressed as:

$$p_{II} = -A_2 x + \frac{B}{2}\ln(x^2 + D) + \frac{E_2}{\sqrt{D}}\omega + c_2^* \tag{10}$$

where

$$A_2 = R_{eq}\left(\frac{m_1 k_1}{R_1^2} + \frac{m_2 k_2}{R_2^2}\right), \quad B = 4k_e, \quad C_2 = R_{eq}\tau_e,$$

$$D = R_{eq}h_o, \quad E_2 = DA_2 - C_2, \quad \omega = \tan^{-1}\frac{x}{\sqrt{D}},$$

$$k_e = k_1\beta_o + k_2(1-\beta_o), \quad \beta_o = \frac{h_{b1}}{h_b} = \frac{h_{o1}}{h_o},$$

$$h_b = h_o + \frac{x_b^2}{R_{eq}}, \quad h_{b1} = h_b - h_{i2}$$

Boundary conditions:

At $x = x_b$, the rolling pressures in zone I and II are identical, i.e., $p_I = P_{II}$, which then gives:

$$A_1 x_b + B_1\ln(x_b^2 + D_1) + C_1\omega_{b1} + c_1^* = -A_2 x_b + \frac{B}{2}\ln(x_b^2 + D) + \frac{E_2}{\sqrt{D}}\omega_b + c_2^* \tag{11}$$

where

$$\omega_b = \tan^{-1}\frac{x_b}{\sqrt{D}}$$

Eq. (11) is derived as:

$$c_2^* = (A_1 + A_2)x_b + B_1\ln(x_b^2 + D_1) - \frac{B}{2}\ln(x_b^2 + D) + C_1\omega_{b1} + c_1^* - \frac{E_2}{\sqrt{D}}\omega_b \tag{12}$$

The specific shear stress $(\tau_m/k_1)_{II}$ in zone II can be obtained as:

$$\left(\frac{\tau_m}{k_1}\right)_{II} = \frac{\Theta_{42} - \Theta_5}{\Theta_3 k_1} \tag{13}$$

where

$$\Theta_{42} = m_2 k_2\left(\frac{x^2}{R_2^2} + 1\right)\frac{2\beta_o x}{R_{eq}} - m_1 k_1\left(\frac{x^2}{R_1^2} + 1\right)\frac{2(1-\beta_o)x}{R_{eq}},$$

$$\Theta_5 = \frac{4\beta_o(1-\beta_o)x^2}{R_{eq}^2}(2k_2 - 2k_1),$$

$$\Theta_3 = \frac{2x}{R_{eq}}\left[\left(\frac{1}{R_1} - \frac{2\beta_o}{R_{eq}}\right)^2 x^2 + 1\right]$$

2.3. Zone III ($x_{n2} \le x \le x_{n1}$), $\tau_e = -m_1k_1 + m_2k_2$

Zone III is the cross shear stress region, and frictions between two rolls and clad sheet are opposite, which is $\tau_e = -m_1k_1 + m_2k_2$.

The rolling pressure distribution in zone III is expressed as:

$$p_{III} = -A_3 x + \frac{B}{2}\ln(x^2 + D) + \frac{E_3}{\sqrt{D}}\omega + c_3^* \tag{14}$$

where

$$A_3 = R_{eq}\left(\frac{-m_1 k_1}{R_1^2} + \frac{m_2 k_2}{R_2^2}\right),$$

$$C_3 = R_{eq}\tau_e = R_{eq}(-m_1k_1 + m_2k_2), \quad E_3 = DA_3 - C_3$$

Boundary conditions:

At $x = x_{n1}$, $p_{II} = p_{III}$

c_3^* in Eq. (14) can be obtained:

$$c_3^* = A^* x_{n1} + E^*\omega_{n1} + c_2^* \tag{15}$$

where

$$A^* = A_3 - A_2, \quad E^* = \frac{E_2 - E_3}{\sqrt{D}}$$

The specific shear stress $(\tau_m/k_1)_{III}$ in zone III can be obtained as:

$$\left(\frac{\tau_m}{k_1}\right)_{III} = \frac{\Theta_{43} - \Theta_5}{\Theta_3 k_1} \tag{16}$$

where

$$\Theta_{43} = -m_2 k_2\left(\frac{x^2}{R_2^2} + 1\right)\frac{2\beta_o x}{R_{eq}} + m_1 k_1\left(\frac{x^2}{R_1^2} + 1\right)\frac{2(1-\beta_o)x}{R_{eq}}$$

2.4. Zone IV ($0 \le x \le x_{n2}$), $\tau_e = -m_1k_1 - m_2k_2$

The rolling pressure distribution in zone IV is expressed as:

$$p_{IV} = -A_4 x + \frac{B}{2}\ln(x^2 + D) + \frac{E_4}{\sqrt{D}}\omega + c_4^* \tag{17}$$

where

$$A_4 = R_{eq}\left(\frac{-m_1 k_1}{R_1^2} - \frac{m_2 k_2}{R_2^2}\right),$$

$$C_4 = R_{eq}\tau_e = R_{eq}(-m_1k_1 - m_2k_2), \quad E_4 = DA_4 - C_4$$

At $x = 0$, $q = q_o$

c_4^* in Eq. (17) can be obtained:

$$c_4^* = 2k_e[1 - \ln D] - q_o \tag{18}$$

The specific shear stress $(\tau_m/k_1)_{IV}$ in zone IV can be obtained as:

$$\left[\frac{\tau_m}{k_1}\right]_{IV} = \frac{\Theta_{44} - \Theta_5}{\Theta_3 k_1} \tag{19}$$

where

$$\Theta_{44} = -m_2 k_2 \left(\frac{x^2}{R_2^2} + 1\right) \frac{2\beta_o x}{R_{eq}} + m_1 k_1 \left(\frac{x^2}{R_1^2} + 1\right) \frac{2(1-\beta_o)x}{R_{eq}}$$

2.5. Determination of the neutral points (x_{n1}, x_{n2})

At $x = x_{n1}$, $p_{II} = p_{III}$

$$-A_2 x_{n1} + \frac{B}{2}\ln(x_{n1}^2 + D) + \frac{E_2}{\sqrt{D}}\omega_{n1} + c_2^* = -A_3 x_{n1} + \frac{B}{2}\ln(x_{n1}^2 + D) + \frac{E_3}{\sqrt{D}}\omega_{n1} + c_3^* \quad (20)$$

At $x = x_{n2}$, $p_{III} = p_{IV}$

$$-A_3 x_{n2} + \frac{B}{2}\ln(x_{n2}^2 + D) + \frac{E_3}{\sqrt{D}}\omega_{n2} + c_3^* = -A_4 x_{n2} + \frac{B}{2}\ln(x_{n2}^2 + D) + \frac{E_4}{\sqrt{D}}\omega_{n2} + c_4^* \quad (21)$$

Combining Eq. (20) with Eq. (21) to get

$$A^* x_{n1} + E^* \omega_{n1} + c_2^* - B^* x_{n2} - F^* \omega_{n2} - c_4^* = 0 \quad (22)$$

where

$$A^* = A_3 - A_2, \quad E^* = \frac{E_2 - E_3}{\sqrt{D}}, \quad B^* = A_3 - A_4,$$

$$F^* = \frac{E_4 - E_3}{\sqrt{D}}, \quad \omega_{n1} = \tan^{-1}\frac{x_{n1}}{\sqrt{D}}, \quad \omega_{n2} = \tan^{-1}\frac{x_{n2}}{\sqrt{D}}$$

there are two unknown (x_{n1}, x_{n2}) in Eq. (22), thus using the principle of volume constancy to get the relationship:

$$x_{n1} = \sqrt{V_A x_{n2}^2 + (V_A - 1)\frac{h_o}{R_A}} \quad (23)$$

where

$$R_A = \frac{V_2}{V_1}, \quad R_A = \frac{1}{R_{eq}} - \frac{h_o}{2R_{eq}^2}$$

By Eqs. (22) and (23), the x_{n1} and x_{n2} can be solved, then c_3^* in Eq. (14) can also be obtained

$$c_3^* = A^* x_{n1} + E^* \omega_{n1} + c_2^* = B^* x_{n2} + F^* \omega_{n2} + c_4^*$$

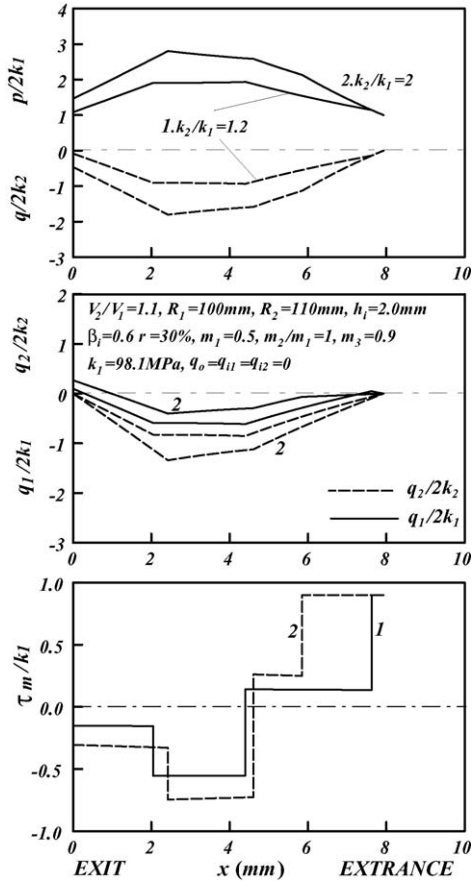

Fig. 4. Various stress distributions for various shear yield stress ratios.

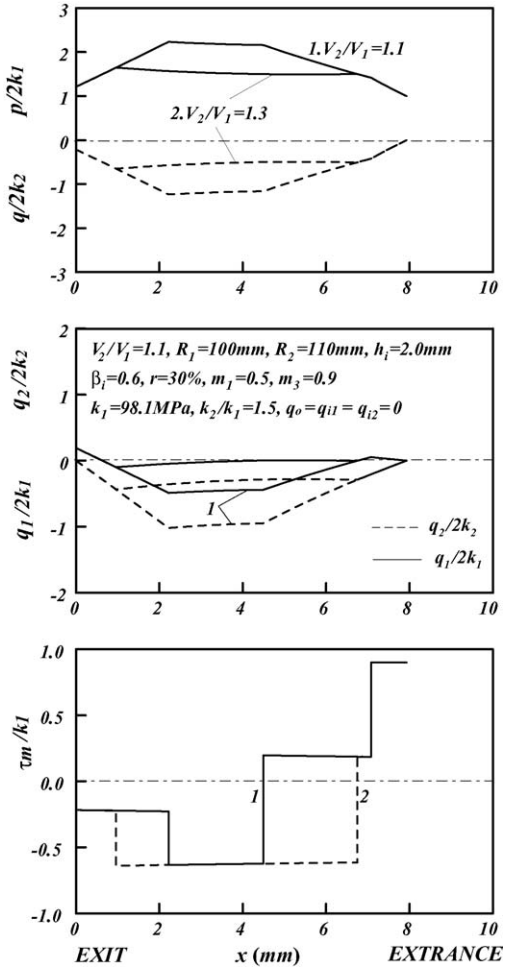

Fig. 5. Various stress distributions for various roll speed ratios.

2.6. Rolling force

Once the mean shear yield stress (k_1 and k_2) and frictional factors (m_1, m_2, and m_3) are known, the rolling force can be found by integrating the normal rolling pressure over the arc length of contact. Thus, the rolling force per unit width, P, is given by:

$$P = \int_0^{x_{n2}} p_{\mathrm{IV}}\,\mathrm{d}x + \int_{x_{n2}}^{x_{n1}} p_{\mathrm{III}}\,\mathrm{d}x + \int_{x_{n1}}^{x_{\mathrm{b}}} p_{\mathrm{II}}\,\mathrm{d}x + \int_{x_{\mathrm{b}}}^{x_{\mathrm{L}}} p_{\mathrm{I}}\,\mathrm{d}x = P_{\mathrm{IV}} + P_{\mathrm{III}} + P_{\mathrm{II}} + P_{\mathrm{I}} \tag{24}$$

2.7. Rolling torque

The rolling torques, T_1 and T_2, exerted by the clad sheet on the upper and lower rolls, respectively, can be calculated by integrating the moment of the roll axis

$$T_1 = R_1\left(-\int_0^{x_{n2}} m_1k_1\,\mathrm{d}x - \int_{x_{n2}}^{x_{n1}} m_1k_1\,\mathrm{d}x + \int_{x_{n1}}^{x_{\mathrm{b}}} m_1k_1\,\mathrm{d}x + \int_{x_{\mathrm{b}}}^{L} m_1k_1\,\mathrm{d}x\right) = R_1m_1k_1(L-2x_{n1}) \tag{25}$$

$$T_2 = R_2\left(-\int_0^{x_{n2}} m_2k_2\,\mathrm{d}x - \int_{x_{n2}}^{x_{n1}} m_2k_2\,\mathrm{d}x + \int_{x_{n1}}^{x_{\mathrm{b}}} m_2k_2\,\mathrm{d}x + \int_{x_{\mathrm{b}}}^{L} m_2k_2\,\mathrm{d}x\right) = R_2m_2k_2(L-2x_{n2}) \tag{26}$$

And the total rolling torque required

$$T = T_1 + T_2 \tag{27}$$

3. Results and discussions

Fig. 4 shows various stress distributions for various shear yield stress ratios (k_2/k_1). As the shear yield stress ratio (k_2/k_1) increases all stresses increase. The bonding point is generated fast for smaller k_2/k_1 ratios. Fig. 5 shows various stress distributions for various roll speed ratios. Increasing the roll speed ratio (V_2/V_1) indicates the roll speed mismatch between the upper and lower rolls is larger; all stress distributions except that τ_{m}/k_1 is slightly changed. The neutral points (x_{n1} and x_{n2}) move towards the entrance and exit, respectively. Fig. 6 shows effects of reduction on x_{n2}/L, x_{n1}/L, x_{b}/L, and β_{o} for various shear yield stress ratios. From this figure, x_{b}/L is decreased as k_2/k_1 increases under the same reduction. It indicates that the smaller k_2/k_1 is helpful

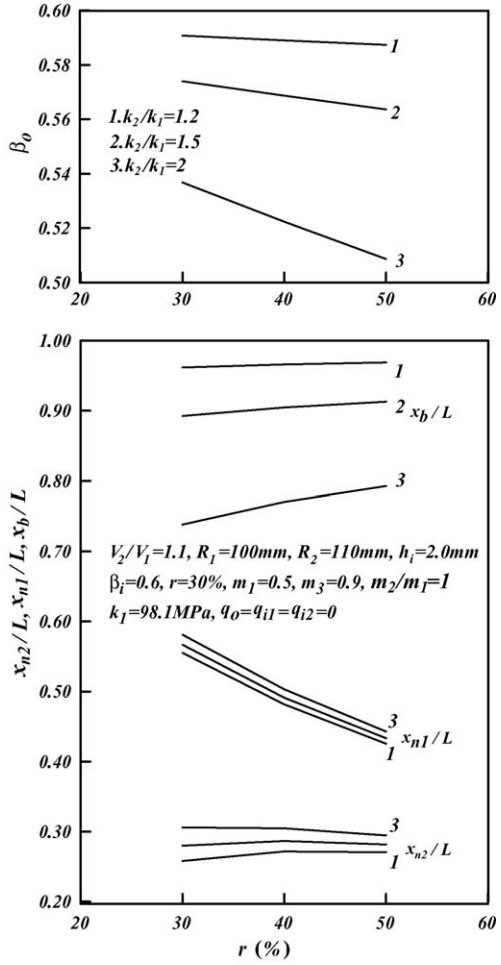

Fig. 6. Effects of reduction on x_{n2}/L, x_{n1}/L, x_{b}/L, and β_{o} for various shear yield stress ratios.

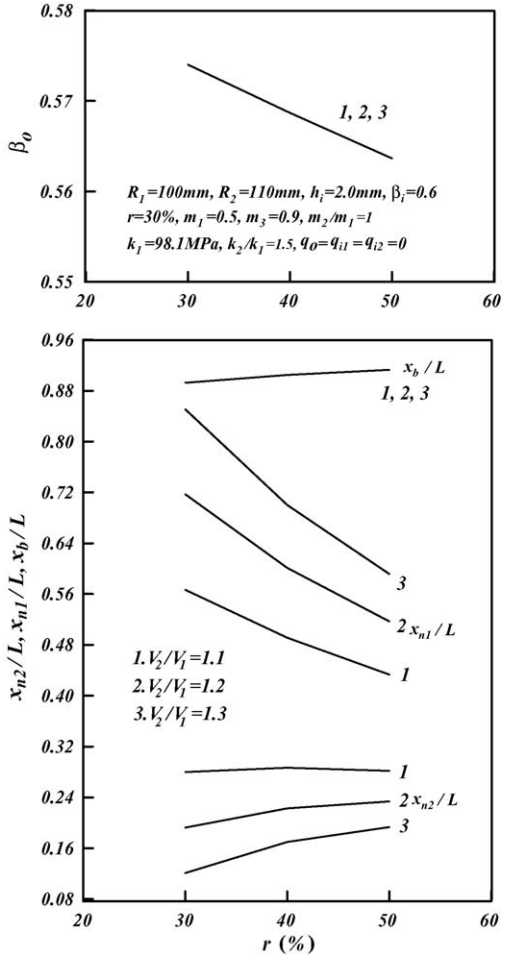

Fig. 7. Effects of reduction on x_{n2}/L, x_{n1}/L, x_{b}/L, and β_{o} for various roll speed ratios.

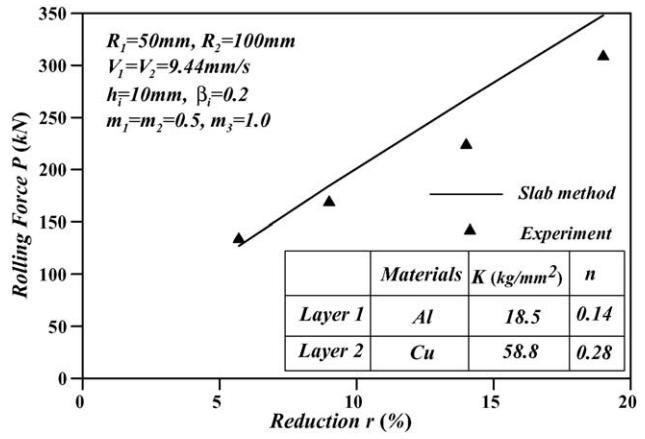

Fig. 8. Comparisons of analysis and experiment for rolling force.

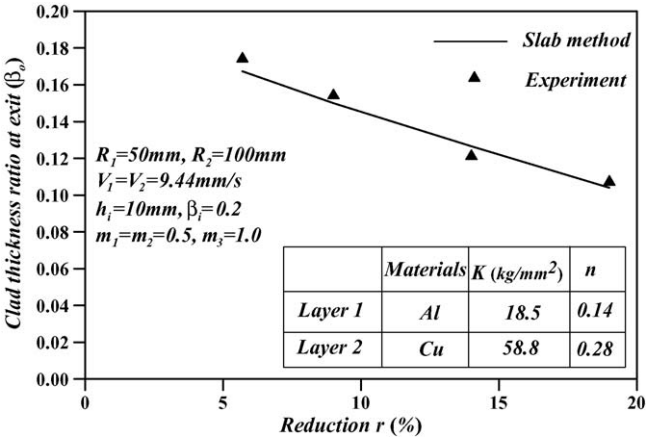

Fig. 9. Comparisons of analysis and experiment for clad thickness ratio.

for the bonding. The thickness ratio at the exit (β_o) under the higher shear yield stress ratio is smaller than that at the entrance (β_i), namely the deformation is heavy after the rolling. It can be seen that x_b/L increases as the reduction increases under the smaller k_2/k_1 ratios, however β_o decreases. Fig. 7 shows effects of reduction on x_{n2}/L, x_{n1}/L, x_b/L, and β_o for various roll speed ratios. From this figure, it reveals that the β_o and x_b/L are not influenced with roll speed ratio (V_2/V_1). As the roll speed ratio increases, x_{n2}/L decreases and x_{n1}/L increases. It indicates that the neutral points (x_{n1} and x_{n2}) move towards the entrance and exit, respectively. Figs. 8 and 9 show comparisons of analysis and experiment for clad thickness ratio and rolling force. Analysis results based on the slab method are in agreement with the experiment [8]. The experiment was carried out to get the clad sheet using Al and Cu materials.

4. Conclusions

The bonding conditions of the unbounded clad sheet asymmetrical rolling have been explored. The important features can be summarized as follows:

1. As reduction, frictional factor at the interface increase, the relative bonding length (x_b/L) increases.
2. It is helpful for the bonding with a smaller shear yield stress ratio.
3. The thickness of clad sheet at the exit (β_o) is always smaller than that at the entrance (β_i) as the upper layer is soft and the lower layer is hard.

References

[1] D. Pan, K. Gao, J. Yu, Cold roll bonding of bimetallic sheets and strips, Mater. Sci. Technol. 5 (1989) 934–939.
[2] S.H. Lee, D.N. Lee, Slab analysis of roll bonding of silver clad phosphor bronze sheets, Mater. Sci. Technol. 7 (1991) 1042–1050.
[3] H. Suzuki, J.I. Araki, K. Shintani, A study on rolling of double-layer metal plate, J. JSTP 13 (1972) 114–121.
[4] H. Suzuki, J.I. Araki, M. Aiba, An analytical study on mechanics in roll bonding of double-layer metal sheets, J. JSTP 15 (1974) 931–937.
[5] M. Kkiuchi, Y.M. Hwang, Mathematical model of complex asymmetrical rolling—study on complex asymmetrical rolling I, J. JSTP 30 (1989) 1308–1315.
[6] M. Kiuchi, Y.M. Hwang, Analysis and experiment on complex asymmetrical rolling—study on complex asymmetrical rolling II, J. JSTP 30 (1989) 1316–1323.
[7] Y.M. Hwang, K. Manabu, Analysis of asymmetrical complex rolling of multi-layer sheets by upper bound method, J. Chin. Soc. Mech. Eng. 13 (1992) 33–45.
[8] Y.M. Huang, T.H. Chen, H.H. Hsu, Analysis of asymmetrical clad sheet rolling by stream function method, Int. J. Mech. Sci. 38 (1996) 443–460.
[9] Y. Jiang, D. Peng, D. Lu, L. Li, Analysis of clad sheet bonding by cold rolling, J. Mater. Process. Technol. 105 (2000) 32–37.
[10] S. Hamauzu, The FEM analysis of hot clad sheet rolling and avoidance of curvature, Iron Steel A 59 (1987) 59–62 (in Japanese).
[11] S. Shiyouya, The analysis of clad sheet rolling by FEM, in: Proceedings of the 40th Joint of Conference of JSTP, 1989, pp. 81–84 (in Japanese).
[12] C. Luo, D. Peng, Z. Xu, Numerical modeling of cold-roll bonding of clad metal sheets, Adv. Technol. Plast. I (1996) 151–158.
[13] Y.M. Hwang, G.Y. Tzou, An analytical approach to asymmetrical cold and hot rolling of clad sheet using the slab method, J. Mater. Process. Technol. 62 (1996) 249–259.